Passive control of linear structures equipped with nonlinear viscous dampers and amplification mechanisms

M. Di Paola, G. Navarra

Dipartimento di Ingegneria Strutturale e Geotecnica

Università degli Studi di Palermo, viale delle Scienze I-90128 Palermo, Italy

Abstract

Fluid damper devices in civil structures such as buildings or bridges are commonly used as energy absorbers for seismic protection. The problem in the response analysis of structures with filled dampers mainly consists in the fact that, due to the strongly nonlinear behavior of such equipments, the response spectrum technique fails. Moreover, in order to enhance the damping effect various toggle brace configurations have been recently proposed.

In this paper by using the concept of power spectral density function compatible with the elastic response spectrum and the stochastic linearization technique, the equivalent damping ratio is obtained. It is shown that once the system is linearized results obtained by Monte Carlo simulation and those obtained by stochastic analysis are in good agreement. Furthermore, various toggle brace configurations are analyzed in detail and compared with a new one here proposed. The analysis is performed by taking into account the inherent nonlinearities of the damper by means of stochastic analysis and validated by using time histories of recorded accelerograms and by the stochastic analysis using spectrum consistent power spectral density.

Introduction

Passive control using energy absorbing devices has received considerable attention in recent years. Among them viscoelastic dampers, fluid dampers, yielding devices have been installed as energy sinks to reduce the structural response and consequent yieldings associated to structural elements during earthquake ground motions [1].

In this paper the attention is focused on viscous fluid damper devices. The appeal of fluid dampers is due to some interesting features: i) low maintenance required; ii) they may be used for several severe earthquakes without damage. Because of these appeals, viscous dampers have found wide application in the shock and vibration isolation of equipment, pipework systems, bridges and buildings.

Attempts of modeling the constitutive laws of viscous fluid dampers may be found in literature by using the classical theory of viscoelasticity [2], or using the fractional derivative equations [3], [4]. Experimental and analytical investigations on seismic response of structures filled with viscous dampers may be found in literature ([5]-[7]). The case of combination of viscous

dampers and seismic isolation has been studied in [8]. Optimal placement of damper to enhance the performance of the whole structure also received considerable attention in recent years ([9]-[19]).

Since the relationship between force and velocity of the damper is highly nonlinear, even supposing that the structure behaves linearly, the whole system damper-structure has inherent nonlinear properties. It follows that the use of Response Spectrum (RS) technique may not be pursued. As a result difficulties arise for design of the damper devices as well as for the evaluation of the response.

In order to overcome this difficulty in [22] a quite different approach has been proposed taking full advantage of stochastic analysis. In order to do this first a piece-wise Power Spectral Density (PSD) function compatible with Response Spectra for different building codes has been found. Then, by using the Statistical Linearization Technique (SLT) ([23]-[26]), the equivalent damping ratio is obtained for Single Degree of Freedom (SDOF) system.

Moreover, the force exerted by damper devices mainly depends on the relative velocity of the joints at which the damper device is installed. Since the structural relative displacements are often small the size of the dampers needs to be large to produce adequate control force, with increasing cost of the damper devices themselves.

In order to reduce the size of the dampers, and then the cost of manufacturing installation of the passive control systems, recently a variety of toggle bracing systems has been proposed to magnify the relative displacement at the end of the damper with an increasing efficiency of the damper itself.

In this frame diagonal and chevron brace configurations have been recently proposed ([7]-[27]). Rotational inertia dampers with toggle bracing for vibration control has been proposed in [28]. Gluck and Ribakov [29] proposed to use diagonals equipped with amplifying braces in which the viscous dampers is connected. Lee et al. [30] extensively studied the various toggle systems including the Gluck and Ribakov scheme taking into account the inherent nonlinearities coming from large interstory displacements.

Comparison between experimental and theoretical studies may be found in [31].

In this paper a new form of amplification mechanism is proposed. Comparison with various toggle brace system existing in literature including the device here proposed is made at a parity of damper inserted to show the performance of such systems. Analysis is conducted with time histories of earthquakes and with the stochastic analysis.

Single degree of freedom system with added viscous damper

In this section the main results exploited in [22] will be briefly summarized for clarity's sake as well as for introducing appropriate notation. The damper effect is an output resistive force, therefore it acts in opposite direction to that of the relative velocity between the ends of the damper device itself. The typical force-velocity relationship is

$$F_D\left(\dot{u}_D\right) = C_D\left|\dot{u}_D\right|^{\alpha}\operatorname{sgn}\left(\dot{u}_D\right) \tag{1}$$

where $\operatorname{sgn}(\cdot)$ is the signum function, C_D and α characterize the damper device. The value of α for seismic applications ranges between 0.10 and 0.50, in this way the viscous force rises very fast for small velocity values and becomes almost constant for large velocity values.

Equation (1) has been validated by laboratory tests performed by manufacturers and research groups. In such laboratory tests the input is a piece-wise constant velocity ranging between fixed values (with opposite sign). The force-velocity diagram for the constitutive law in eq. (1) for $u\left(t\right) = A\sin\left(\Omega t\right)$ are reported in Figure 1-a for four different values of α. In Figure 1-b the corresponding force-displacement diagrams are plotted showing the typical hysteretic behavior of the damper device.

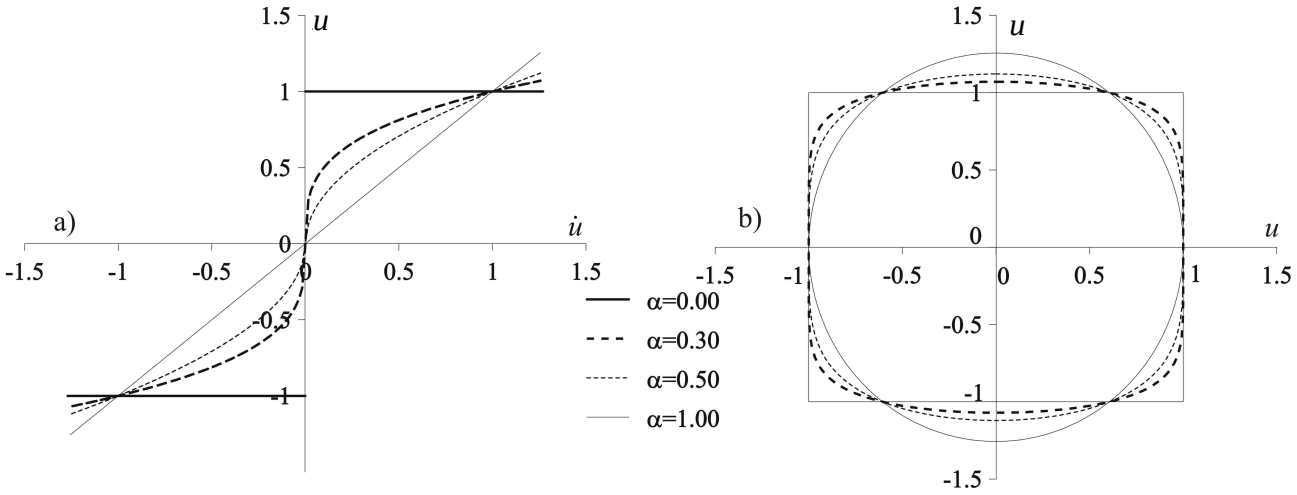

Figure 1. Damper device constitutive law for $u_D\left(t\right) = A\sin\left(\Omega t\right)$, for different values of α and C_D=1, A=1; a) force-velocity relationship; b) force-displacement relationship.

It is to be remarked that for α=1 the damper is linear and the force-displacement plot is an ellipse, while for α=0 the constitutive law of pure friction device is restored and the force-displacement plot is a rectangle.

Let us now consider the one-story shear-type building shown in Figure 2 subjected to ground acceleration $\ddot{z}_g\left(t\right)$ modeled as a zero mean normal process. It follows that the displacement and its derivative are stochastic processes too, and as customary, we will denote them with capital letter, that is $u\left(t\right)$ will be replaced by $U\left(t\right)$, $\ddot{z}_g\left(t\right)$ by $\ddot{Z}_g\left(t\right)$ and so on.

The global stiffness of the columns of the SDOF model is K, the mass is M, the structural damping coefficient is denoted as $C^{(s)}$. Moreover, let θ be the angle of the brace armed with the damper device characterized by C_D and α, the dynamic equilibrium of the top mass is written as

$$\ddot{U}\left(t\right) + \eta\left|\dot{U}\left(t\right)\right|^{\alpha}\operatorname{sgn}\left(\dot{U}\left(t\right)\right) + 2\zeta^{(s)}\omega_0\dot{U}\left(t\right) + \omega_0^2 U\left(t\right) = -\ddot{Z}_g\left(t\right) \tag{2}$$

where $U\left(t\right)$ is the relative displacement, $\eta = C_D\left|\cos\theta\right|^{\alpha+1}/M$, $\zeta^{(s)} = C^{(s)}/2M\omega_0$ is percentage of critical damping and $\omega_0 = \sqrt{K/M}$ is the natural radian frequency.

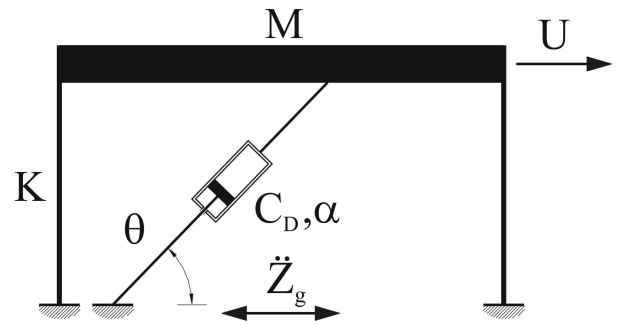

Figure 2. One-story shear-type building model excited by ground acceleration.

Due to the presence of the damper device, the response process is non Gaussian. According to the Stochastic Linearization Technique (SLT) the original system, ruled by eq.(2), is replaced by a linear equivalent one as follows

$$\ddot{U}(t)+2\zeta^{(e)}\omega_0\dot{U}(t)+\omega_0^2U(t)=-\ddot{Z}_g(t) \tag{3}$$

where the superscript *(e)* in parenthesis means equivalent. The parameter $\zeta^{(e)}$ is chosen in such a way that the mean square error made in passing from eq.(2) to eq.(3) is minimum with respect to $\zeta^{(e)}$, that is

$$\mathrm{E}\left[\left(\eta\left|\dot{U}\right|^{\alpha}\operatorname{sgn}\left(\dot{U}\right)+\left(\zeta^{(s)}-\zeta^{(e)}\right)\dot{U}\right)^2\right]=\min_{\zeta^{(e)}} \tag{4}$$

where E[·] means ensemble average. By performing the minimum we get

$$\zeta^{(e)}=\zeta^{(s)}+\eta\frac{E\left[\left|\dot{U}\right|^{\alpha+1}\right]}{E\left[\dot{U}^2\right]} \tag{5}$$

In view of the assumed Gaussianity of the response of eq.(3), equation (5) proves to be equivalent to

$$\zeta^{(e)}=\zeta^{(s)}+\eta E\left[\left|\dot{U}\right|^{\alpha-1}\right] \tag{6}$$

Since the nonlinear system represented by eq.(2) has been replaced by the linear one, then the response of eq.(3) is Gaussian; it follows that

$$\mathrm{E}\left[\left|\dot{U}\right|^{\gamma}\right]=\frac{2}{\sqrt{2\pi}\sigma_{\dot{U}}}\int_0^{\infty}\exp\left(-\frac{\dot{u}^2}{2\sigma_{\dot{U}}^2}\right)\dot{u}^{\gamma}\,\mathrm{d}\,\dot{u}=\frac{2^{\frac{1+\gamma}{2}}\Gamma\left(\frac{1+\gamma}{2}\right)}{\sqrt{2\pi}}\sigma_{\dot{U}}^{\gamma}\ ;\ (\gamma=\alpha+1,\ \gamma=2\text{ or }\gamma=\alpha-1) \tag{7}$$

where $\Gamma(\cdot)$ is the gamma function and $\sigma_{\dot{U}}=\sqrt{E\left[\dot{U}^2\right]}$ is the standard deviation of the velocity $\dot{U}$. It follows that by using eq.(5) ($\gamma=\alpha+1$)

$$\zeta^{(e)}=\zeta^{(s)}+\eta\frac{2^{1+\frac{\alpha}{2}}\Gamma\left(1+\frac{\alpha}{2}\right)}{\sqrt{2\pi}}\sigma_{\dot{U}}^{\alpha-1} \tag{8}$$

At this stage two different kind of analyses may be performed: i) we may assume that the seismic input is modeled as a non stationary one, then by using some step-by-step analysis [32] the response variance may be easily performed. In this case at each temporal step the equivalent damping $\zeta^{(e)}$ must be evaluated and the maximum peak of the response will be evaluated by using approximate techniques [33]; ii) both the seismic input and the response are considered as a segmented stationary process. In this case the analysis is very simple and the parameter $\zeta^{(e)}$ remains constant. Moreover the maximum peak may be evaluated with the Vanmarcke formulation [34] in the finite duration T_S. In both cases the input will be chosen as a spectrum consistent one in order to have, at least for a single-degree-of-freedom linear oscillator, comparable results.

Since the main goal of the present paper is readily finding the amount of the equivalent damping ratio for both design of viscous equipments and evaluation of the stress level in the structure, the stationary model will be selected.

In view of the assumed Gaussianity and stationarity both input $\ddot{Z}_g(t)$ and output $U(t)$ processes are fully characterized in probabilistic setting by the (one sided) PSD, denoted as $G_{\ddot{Z}_g}(\omega)$ and $G_U(\omega)$, respectively.

Once the finite duration T_S is selected, the PSD of the process $\ddot{Z}_g(t)$ is modulated in such a way that the corresponding Response Spectrum is compatible with the assigned one by the building code selected (see [22]). In this way at least for a single degree of freedom linear system, results in terms of maximum response peak by stochastic analysis and by using RS technique are almost identical. It is worth noting that the PSD of the ground acceleration is independent on the behavior of the superimposed structure and then it may be used for both linear and non linear ones.

From eq.(8) one realizes that $\zeta^{(e)}$ depends on $\sigma_{\dot{X}}$, that is still unknown because it implicitly depends on $\zeta^{(e)}$, then, in general, an iterative procedure is necessary. In the first attempt one fixes an arbitrary value of $\zeta^{(e)}$, by using this value the variance of velocity may be easily evaluated as

$$\sigma_{\dot{U}}^2 = \int_0^\infty G_{\dot{U}}(\omega)\, d\omega = \int_0^\infty \omega^2 G_U(\omega)\, d\omega = \int_0^\infty \omega^2 G_{\ddot{Z}_g}(\omega) \left|H(\omega)\right|^2 d\omega \tag{9}$$

where $H(\omega)$ is the transfer function of eq.(3)

$$H(\omega) = \left(\omega_0^2 - \omega^2 + 2i\zeta^{(e)}\omega_0\omega\right)^{-1} \tag{10}$$

i being the imaginary unit. By inserting $\sigma_{\dot{U}}$ evaluated by eq.(9) a new attempt of $\zeta^{(e)}$ is readily found by eq.(8) and so on. The procedure ends when the values of $\zeta^{(e)}$ between two successive iterations are practically coincident.

An approximation of $\sigma_{\dot{U}}$ may be obtained by the expression

$$\sigma_{\dot{U}}^2 \cong \frac{\pi G_{\ddot{Z}_g}(\omega_0)}{4\zeta^{(e)}\omega_0} \tag{11}$$

By inserting eq. (11) in eq.(8), an approximation of $\zeta^{(e)}$ is found as

$$\zeta^{(e)} = \zeta^{(s)} + \eta\rho(\alpha)\left(\frac{G_{\ddot{Z}_g}(\omega_0)}{\zeta^{(e)}\omega_0}\right)^{\frac{\alpha-1}{2}};\ \rho(\alpha) = \Gamma\left(1+\frac{\alpha}{2}\right)\sqrt{2^{3-\alpha}\pi^{\alpha-2}} \tag{12-a,b}$$

By solving the nonlinear algebraic equation (12-a) a good estimate of $\zeta^{(e)}$ is readily found useful for design purposes how already discussed in [22].

The maximum peak of displacement for the Gaussian steady-state response of eq.(3) may be evaluated by Vanmarcke formulation [34] stating that the maximum peak is given by

$$E\left[\left|U_{max}\right|\right]_{T_S} = \sqrt{\lambda_{U,0}}\sqrt{2\ln\left\{2\nu(T_S)\left[1-\exp\left(-\delta^{1.2}\sqrt{\pi\ln 2\nu(T_S)}\right)\right]\right\}} \tag{13}$$

where the parameter ν and the spread factor δ of the process are given as

$$\nu(T_s) = \frac{T_s}{2\pi}\sqrt{\frac{\lambda_{U,2}}{\lambda_{U,0}}}(-\ln 0.5)^{-1};\qquad \delta = \sqrt{1-\frac{\lambda_{U,1}^2}{\lambda_{U,0}\lambda_{U,2}}} \tag{14}$$

with the spectral moments $\lambda_{U,j}$ expressed as

$$\lambda_{U,j} = \int_0^\infty \omega^j G_U(\omega)d\omega \tag{15}$$

If $G_{\ddot{Z}_g}(\omega)$ is compatible with the RS, then eq.(13) coincides with the RS in terms of displacements. If we would evaluate the RS in terms of velocity, we may use the same eq.(13) simply by substituting $\lambda_{U,j}$ with $\lambda_{U,j+2}$

Various geometric configuration of toggle brace systems

Let us consider the diagonal and chevron brace configuration as shown in Figure 3. Let us denote as *u* the interstory drift and u_D the relative displacement along the axis of the damper. Moreover following [7] we denote *f* as a magnification factor depending on the toggle brace configuration

$$u_D = f\cdot u;\ (f \geq 0). \tag{16}$$

The horizontal component of the force F_D exerted by the damper on the frame is then given as

$$F = f\cdot F_D. \tag{17}$$

Now let us suppose that the force at the end of the damper is expressed as in eq.(1), then $F_D(\dot{u}_D) = C_D\left|\dot{u}_D\right|^\alpha \operatorname{sgn}(\dot{u}_D)$. By inserting eq.(16) in eq.(1) and taking into account eq.(17), the force exerted on the top mass of the frame results

$$F = f\cdot C_D\left|\dot{u}_D\right|^\alpha \operatorname{sgn}(\dot{u}_D) = f^{1+\alpha}C_D\left|\dot{u}\right|^\alpha \operatorname{sgn}(\dot{u}). \tag{18}$$

In Figure 3 different configurations of the dampers proposed in literature with the corresponding magnification factors are presented and compared with the proposed one in terms of magnification factor, reported in Figure 3-f. It mainly consists in a simple pendulum hinged at the top mass (point

A), that is hinged at the two diagonal (BD and BE) fixed at the bottom floor (points D and E). The dampers are installed at the free end of the pendulum at the bottom floor. The magnification factor hence depends on the ratio *b/a* that may be assumed 5÷7.

In the next section the comparison between the various configuration in terms of capability to reduce structural response are reported.

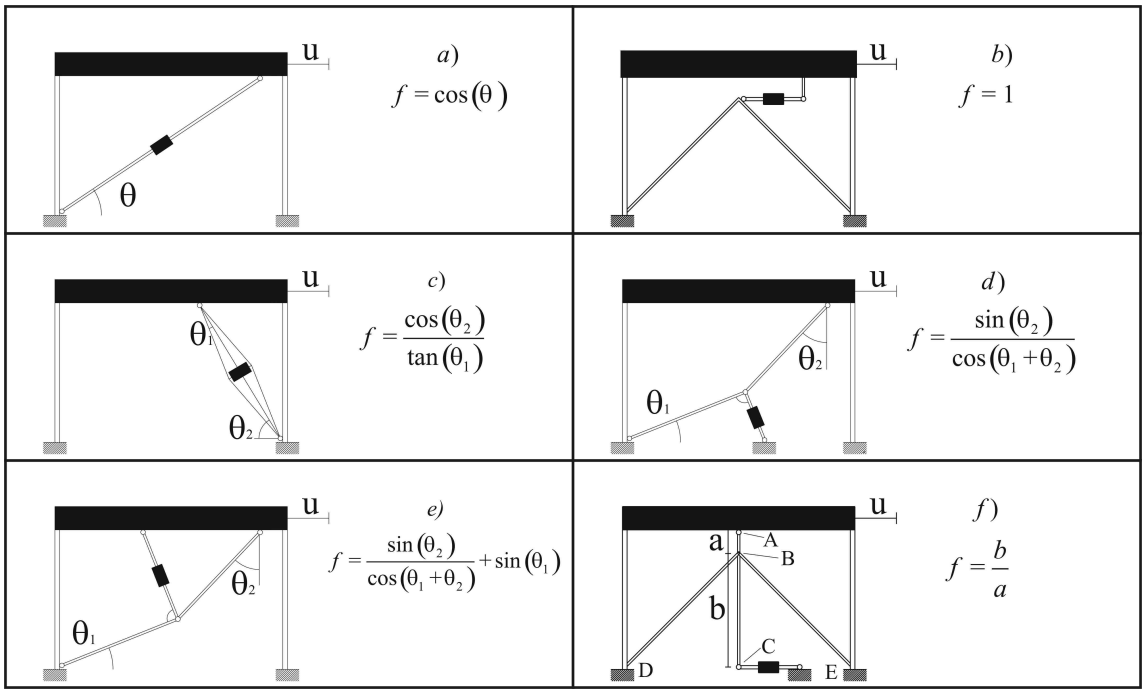

Figure 3. Different configuration of toggle brace; a) simple brace; b) chevron brace; c) scissor-jack toggle system in [2]; d) lower toggle brace in [1]; e) upper toggle brace in [1]; f) proposed configuration.

Numerical applications

In this section applications to one storey building model are presented in order to asses the validity of the SLT as well as of approximations made in eqs.(12). Moreover, in order to show the effectiveness of the proposed mechanism, some stochastic and deterministic analyses varying the toggle brace configuration have been reported.

Effectiveness of SLT

In order to verify the effectiveness of SLT, for shortness's sake, hereinafter only results obtained by the RS proposed by the Eurocode 8 with soil type B, category 2 (a_g=0.25g) are reported, but the analyses conducted for other categories and soil types give always comparable results. For this kind of RS, the compatible one-sided PSD, $G_{\ddot{Z}_g}(\omega)$, has the expression reported in [22]. In all the cases it has been assumed $\zeta^{(s)}=0.05$.

Direct approach of the nonlinear eq.(2) has been performed by means of Monte Carlo method by generating the ground acceleration $\ddot{Z}_g(t)$ by means of the well known expression

$$\ddot{Z}_g(t) = \sum_{k=1}^{p} \sqrt{2G_{\ddot{Z}_g}(\omega_k)\Delta\omega}\cos(\omega_k t + \Psi_k) \tag{19}$$

where the value of $\Delta\omega$ selected is 0.25 rad/sec, the total number of harmonic waves *p* is 600, so that the cut-off frequency is 150 rad/sec. In eq.(19) Ψ_k are random phase angles uniformly distributed in 0-2π.

All the step-by-step nonlinear analyses have been performed by generating 500 samples of artificial accelerograms of T_S=30 sec, making the analyses and averaging results in terms of absolute maximum peak. In order to avoid transient effects the initial conditions on the state variables of the response for the k-th sample function has been assumed as the state at the end of the (k-1)-th sample function of the response. The stochastic analysis in terms of absolute maximum peak of displacements and velocity is conducted via Vanmarcke method [34].

Some results for the SDOF model already obtained in [22] are here re-proposed for completeness's sake.

In Figure 4 the equivalent damping ratio $\zeta^{(e)}$ versus ω_0 is performed by eq.(12), and by using the iterative procedure previously described, for different values of η and different values of parameter α. From these figures appears that eq.(12) follows sufficiently well the trend of the equivalent damping obtained by using the SLT.

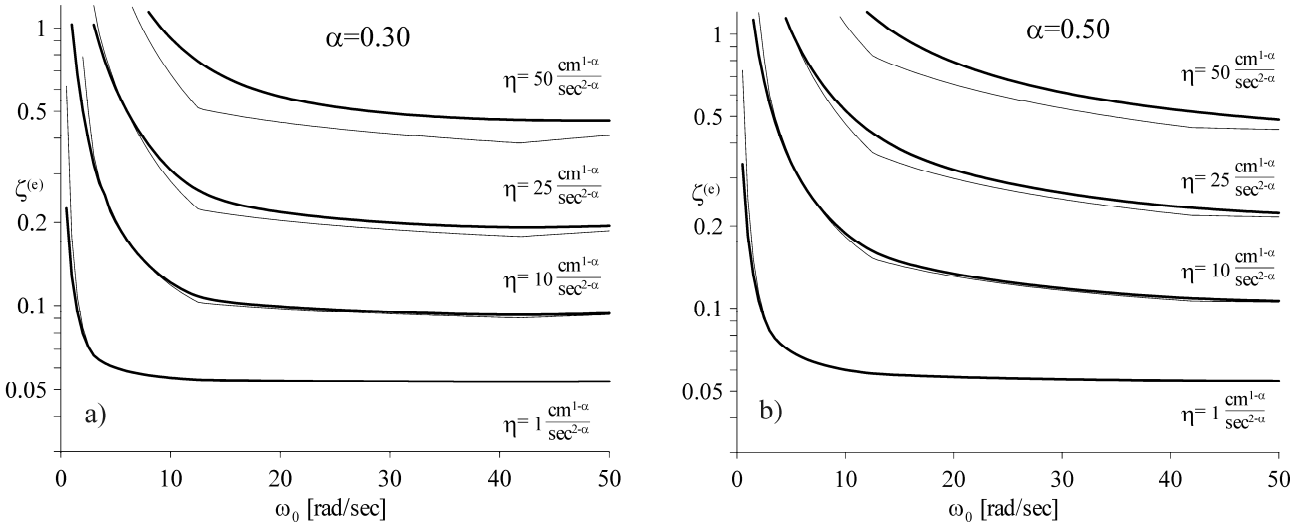

Figure 4. Equivalent damping ratio due to damper device versus ω_0, for different values of η and α: eq.(12-a) (solid line); iterative procedure (bold line); a) α=0.3; b) α=0.5.

In Figure 5 the RS in terms of displacement are plotted for different values of η and for two different values of α. The RS in terms of velocity and acceleration have been also obtained showing a similar behavior and are not here reported for shortness's sake.

The RS have been evaluated: i) by means of the Monte Carlo simulation on linearized equation with the $\zeta^{(e)}$ obtained by SLT (when the convergence for each value of $T_0 = 2\pi/\omega_0$ has been achieved); ii) using the Vanmarcke method on the linearized system; iii) by Monte Carlo simulation directly integrating the nonlinear equation of motion.

From these figures it appears that once $\zeta^{(e)}$ is evaluated all the analysis methods are in good agreement each other in terms of the maximum peak of the response. If the nonlinear term increases, that is the smaller α and the bigger η, for high values of the period T_0 the accuracy of results conducted by the SLT and approximation of eq.(12) decreases, the maximum error is obtained for η= 25 cm$^{1-\alpha}$/sec$^{2-\alpha}$ and is of order of 7%.

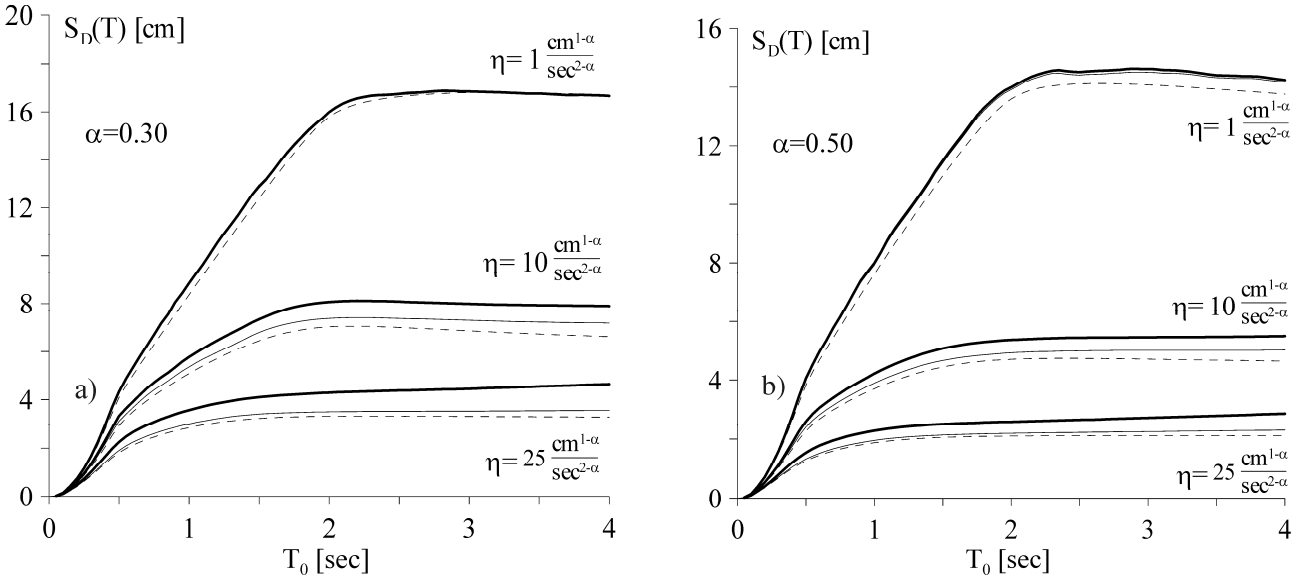

Figure 5. Response Spectrum in terms of displacement; dashed line stochastic analysis; solid line Monte Carlo simulation performed on eq.(3); bold line Monte Carlo simulation performed on eq.(2); a) α=0.30; b) α=0.50.

Toggle brace mechanisms

In this section results from dynamic analyses of a single-degree-of-freedom system have been reported. From the reference structure model available in [17] for the computer code SAP2000, the following dynamic properties of the SDOF system have been derived: $M = 9.12\,\mathrm{Ns^2/mm}$, $K = 5647.1\,\mathrm{N/mm}$, $\omega_0 = 24.886\,\mathrm{rad/s}$. Moreover, the structural damping ratio has been set as $\zeta^{(s)} = 0.04$. Two different cases have been analyzed, that is the damper behaves linearly and the damper has a nonlinear constitutive law.

In order to highlight the effectiveness of the amplification mechanism we start with a structural damping $\zeta^{(s)} = 0.04$, and we insert a damper that, with $f = 1$ (case *b* of Figure 3), the total amount of damping is increased only of 0.01. It will be shown that by using mechanism to amplify the relative displacements (and velocities) at the end of the damper, the increase of the total damping may result consistent.

In the case that the damper exhibit a linear relation between velocity and exerted force (α=1), the damping amount provided by the damper and the structural damping are additive. In this case the eq.(6), taking into account eq.(18), may be rewritten as

$$\zeta^{(e)} = \zeta^{(s)} + \frac{C_{D,lin} f^2}{2M\omega_0} \quad . \tag{20}$$

From eq.(20) the parameter $C_{D,lin} = 5.44\,\mathrm{Ns/mm}$.

In the nonlinear case (α=0.30) the increment of the damping is not additive and then the criterion to select the parameter $C_{D,nl}$, that only increase the total damping of 0.01 with $f=1$, has to be evaluated with the aid of the iterative procedure described in the previous section.

In order to obtain a total damping ratio equal to $\zeta^{(e)}=0.05$, a value of $C_{D,nl}=126.8\,\mathrm{Ns}^{\alpha}/\mathrm{mm}^{\alpha}$ is found with reference to a ground motion modeled as a zero mean Gaussian process having a power spectral density function coherent with Eurocode 8, soil type "B" and peak ground acceleration equal to 0.25 times the gravity acceleration.

The SDOF system has been subjected both to stochastic and deterministic analyses, as described in the following, in order to show the effectiveness of the various configuration to reduce the structural response. The magnification factors f for the various configuration have been derived from [7] and [27] for upper toggle, lower toggle and scissor-jack toggle; for the proposed configuration a magnification factor $f=5$ has been selected.

Stochastic analyses. In Table 1 for each configuration the results in terms of standard deviation of the displacement and mean value of absolute peaks are reported for Monte Carlo simulation and Stochastic Analysis in the case of linear damper. Following the iterative procedure summarized in the previous sections, for each configuration and referring to a ground motion coherent with Eurocode 8, soil type "B" and a_g= 0.25g an equivalent damping ratio has been estimated. Hence, taking full advantage from the stochastic analysis tools, the standard deviation and the mean value of the absolute peaks of the response have been computed for the linearized system.

			Monte Carlo Simulation		Stochastic Analysis	
Configurations	f	$\zeta^{(e)}$	σ_U [mm]	$E\left[\lvert U_{max}\rvert\right]_{T_s}$ [mm]	σ_U [mm]	$E\left[\lvert U_{max}\rvert\right]_{T_s}$ [mm]
Uncontrolled	-	4.0%	4.078	13.272	3.980	12.772
Chevron brace	1.00	5.0%	3.665	12.053	3.559	11.518
Scissor-jack toggle	2.16	8.0%	2.939	9.843	2.814	9.246
Lower toggle	2.66	11.1%	2.530	8.538	2.390	7.923
Upper toggle	3.19	14.2%	2.261	7.663	2.113	7.045
Proposed	5.00	29.0%	1.638	5.545	1.478	4.986

Table 1. Standard deviation of the displacement and mean value of the absolute peaks of the response (EC8 – soil "B", a_g=0.25g); linear damper ($C_{D,lin}=5.44\,\mathrm{Ns/mm}$, α=1.00).

These results may be compared with those obtained by a Monte Carlo simulation over 20000 samples of the response displacement with a duration of 30 s. These response samples have been obtained using a fourth-order Runge-Kutta integration scheme on a differential equation like the one reported in eq.(2) in which $\ddot{Z}_g(t)$ is modeled as a zero mean Gaussian process with a PSD function coherent with Eurocode 8, soil type "B" and ag= 0.25g. In Table 2 the same results are reported with reference to the case in which the damper has a nonlinear behavior.

In both linear and nonlinear cases the results obtained from Monte Carlo simulation are very close with those obtained from stochastic analysis on the linearized system, thus proving the effectiveness of the stochastic linearization technique. Moreover, the increasing of the equivalent

damping ratio shows the utility of amplification mechanisms to enhance the performance of fluid dampers. In fact, while the damper in the chevron configuration in all the cases provide a reduction of 10-11% of structural response (in terms of both standard deviation and mean value of absolute peak of displacements), the proposed configuration reduce the response of 60% in the linear case and of 45% in the nonlinear case.

			Monte Carlo Simulation		Stochastic Analysis	
Configurations	f	$\zeta^{(e)}$	σ_U [mm]	$E\left[\lvert U_{max}\rvert\right]_{T_S}$ [mm]	σ_U [mm]	$E\left[\lvert U_{max}\rvert\right]_{T_S}$ [mm]
Uncontrolled	-	4.0%	4.079	13.255	3.980	12.772
Chevron brace	1.00	5.0%	3.663	12.264	3.559	11.518
Scissor-jack toggle	2.16	6.7%	3.181	11.021	3.067	10.026
Lower toggle	2.662	8.3%	2.893	10.251	2.770	9.109
Upper toggle	3.191	9.7%	2.683	9.676	2.556	8.442
Proposed	5.00	16.2%	2.116	7.977	1.975	6.602

Table 2. Standard deviation of the displacement and mean value of the absolute peaks of the response (EC8 – soil "B", a_g=0.25g); nonlinear damper ($C_{D,nl} = 126.8\,\mathrm{Ns}^{\alpha}/\mathrm{mm}^{\alpha}$, α=0.30).

Deterministic analyses. In order to test the effectiveness of the toggle brace mechanisms in the reduction of the structural response even when the acceleration is non stationary, four historical recorded ground motion time histories have been selected.

Configurations	f	El Centro [mm]	Kobe [mm]	Newhall [mm]	Santa Monica [mm]
Uncontrolled	-	11.717	8.185	15.656	6.961
Chevron brace	1.00	10.961	7.646	14.514	6.210
Scissor-jack toggle	2.16	8.941	6.144	11.738	5.350
Lower toggle	2.662	7.987	5.626	10.491	4.963
Upper toggle	3.191	7.010	5.173	9.252	4.529
Proposed	5.00	4.712	3.877	6.423	3.047

Table 3. Absolute peaks of the response for historical earthquakes; linear damper ($C_{D,lin} = 5.44\,\mathrm{Ns/mm}$, α=1.00).

The earthquake excitations used consisted of the El Centro, component S00E; the Kobe, component EW; the Newhall, at LA County Fire Station, component 90°, the Santa Monica at City Hall, component 0°. All the selected excitation have been scaled in such a way that the peak ground acceleration is equal to 0.25 times the gravity acceleration.

The displacement time histories of the system have been obtained using a fourth-order Runge-Kutta integration scheme on a differential equation like the one reported in eq. (2) and in Table 3 and Table 4 the absolute peaks of the displacements for all the configuration and for the selected earthquakes are reported in the cases of linear damper and nonlinear damper, respectively.

In Figure 6 and Figure 7 the response displacement for the uncontrolled configuration, upper toggle brace and the proposed configuration have been reported for comparison in the cases of linear damper and non linear damper, respectively.

Configurations	f	El Centro [mm]	Kobe [mm]	Newhall [mm]	Santa Monica [mm]
Uncontrolled	-	11.717	8.185	15.656	6.961
Chevron brace	1.00	10.959	7.600	14.855	6.110
Scissor-jack toggle	2.16	9.849	6.616	13.643	5.604
Lower toggle	2.662	9.401	6.172	13.106	5.411
Upper toggle	3.191	8.964	5.803	12.518	5.207
Proposed	5.00	7.523	4.961	10.639	4.399

Table 4. Absolute peaks of the response for historical earthquakes; nonlinear damper.
($C_{D,nl} = 126.8\,\mathrm{Ns}^{\alpha}/\mathrm{mm}^{\alpha}$, α=0.30)

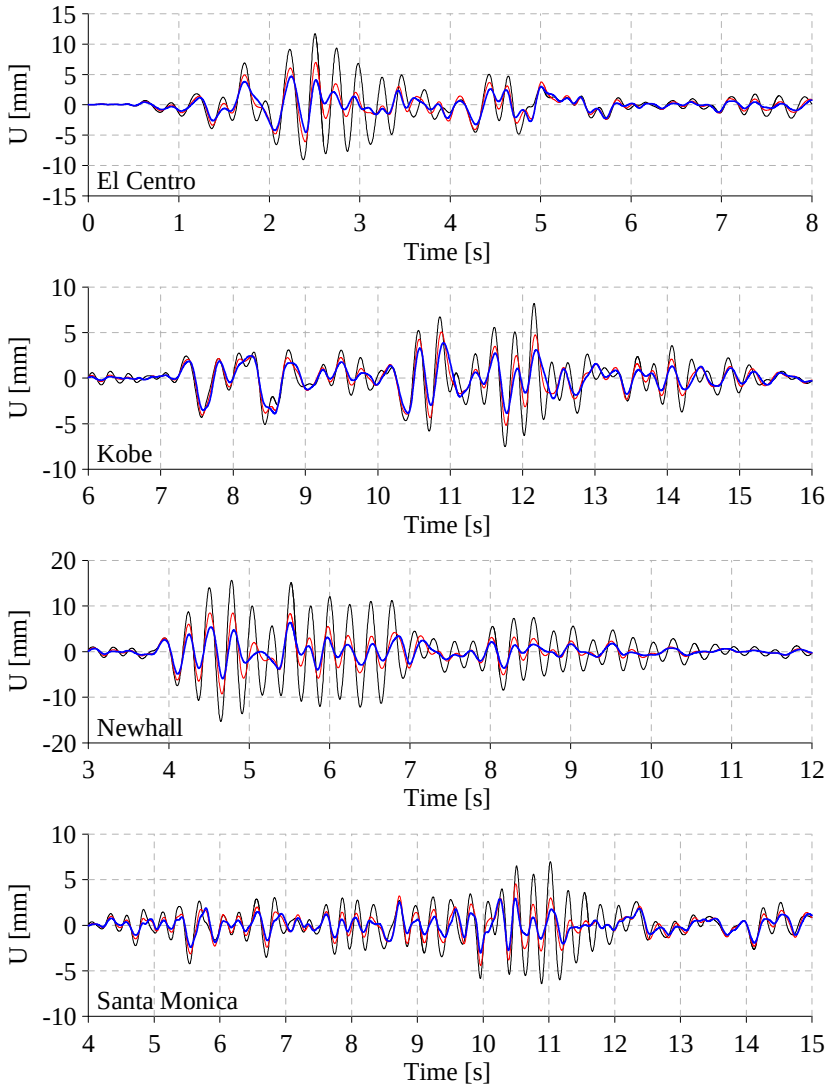

Figure 6. Displacements time histories under the selected earthquakes: uncontrolled system (black line), upper toggle brace (red line); proposed configuration (solid blue line); linear damper ($C_{D,lin} = 5.44\,\mathrm{Ns/mm}$, α=1.00).

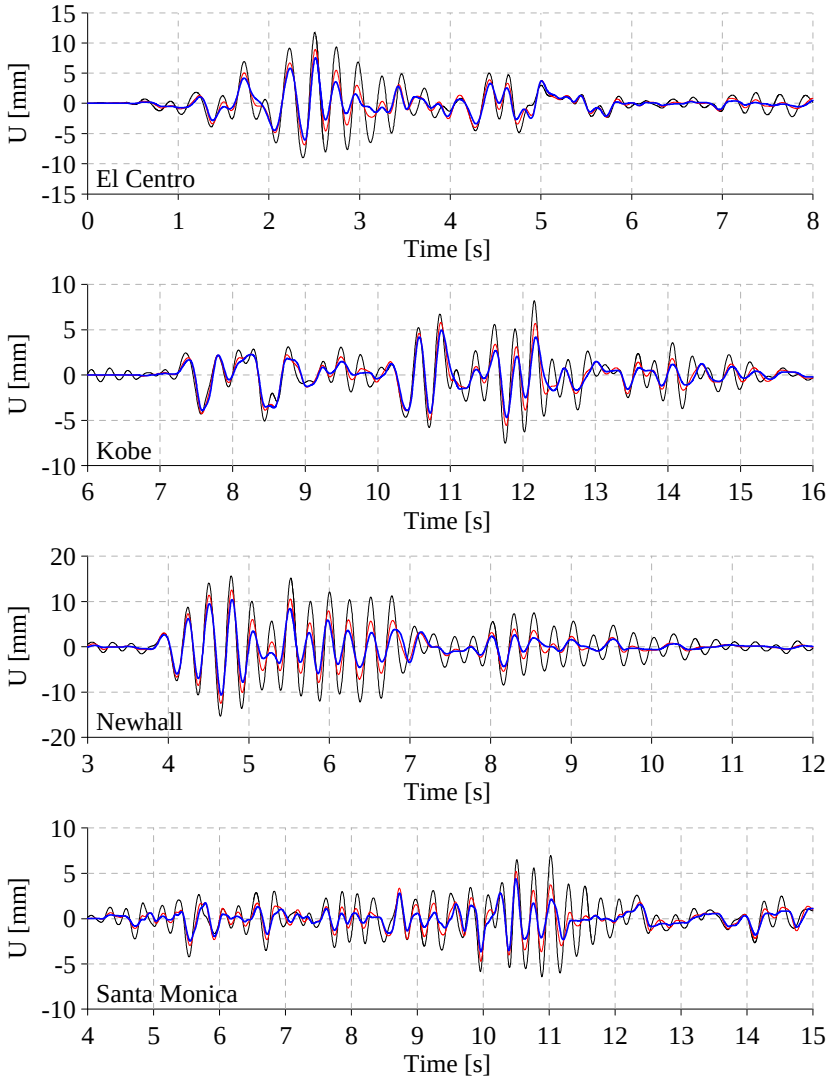

Figure 7. Displacements time histories under the selected earthquakes: uncontrolled system (black line), upper toggle brace (red line); proposed configuration (solid blue line); nonlinear damper ($C_{D,nl} = 126.8\,\mathrm{Ns}^{\alpha}/\mathrm{mm}^{\alpha}$, α=0.30).

Conclusions

Passive control strategy of structures under earthquake ground motions by using viscous damper devices may be enhanced by inserting the viscous damper in a mechanism that increases the relative displacement at the end of the damper itself. The seismic acceleration has been modeled as a zero mean normal stationary process characterized by a power spectral density function compatible with the assigned response spectrum. It has been shown that results provided by the statistic linearization give a very good estimation of the peak response of the structural system.

It has been also shown that, once the equivalent damping ratio is obtained by the statistic linearization, the analysis performed by using the reduced response spectrum technique gives acceptable results.

In this paper various mechanisms already proposed in literature have been analyzed in detail by using accelerograms of severe earthquakes and by using stochastic analysis with power spectral

density compatible with power spectra. The results take into account the inherent nonlinearities of the viscous dampers.

All the results are compared with a new mechanism here proposed that is composed by a pendulum hinged at the upper floor and with two braces fixed at the bottom floor. It is shown that in all the cases, at a parity of damper installed, the proposed mechanism has a better performance with respect to the other ones existing in literature.

References

[1] Jeronimo E, Guerreiro L. Seismic displacement analysis of bridges with viscous dampers. Proc., 12th European Conference on Earthquake Engineering, 2002; Paper reference 373.

[2] Schwann KJ, Reinsch HH, Weber FM. Description of the feature of viscous dampers on the goals of equivalent rheological models, presented for pipework dampers. *Proc. pres. vess. piping conf.*, ASME, 1988; 127, 477-484.

[3] Kijewski T, Kareem A. Analysis of full-scale data from a tall building in Boston: damping estimates. *Proc. of 10th ICWE,* 1999; Copenhagen, June 21-24, I, Elsevier.

[4] Makris N, Constantinou MC, Dargush GF. Analytical model of viscoelastic fluid dampers. *Journal of Structural Engineering, ASCE,* 1993; 119(11), 3310-3325.

[5] Constantinou MC, Symans MD. Experimental and analytical investigation of seismic response of structures with supplemental viscous dampers. *Tech. Rep. NCEER-92-0032*, National Center for Earthquake Engineering Research, Buffalo, N.Y., 1992.

[6] Chang KC, Lai ML, Soong TT, Hao DS, Yeh YC. Seismic behavior and Design Guidelines for steel frames structures with added viscoelastic dampers. *Tech. Rep. NCEER-93-0009*, National Center for Earthquake Engineering Research, Buffalo, N.Y., 1993.

[7] Constantinou MC, Tsopelas P, Hammel W, Sigaher AN. Toggle brace damper seismic energy dissipation system. *Journal of Structural Engineering-ASCE*, 2001; 127(2), 105-112.

[8] Makris N., Constantinou MC. Spring-viscous dampers systems for combined seismic and vibration isolation. *Earthquake Engineering Structural. Dynamics,* 1992; 21, 649-664.

[9] Ashour SA, Hanson RD. Elastic seismic response of buildings with supplemental damping. *Rep. No. UMCE87-01*, Department of Civil Engineering, University of Michigan, Ann Arbor, MI., 1987.

[10] Velestos AS, Ventura CE. Modal analysis of non proportionally damped linear systems *Earthquake Engineering Structural. Dynamics*, 1986; 14, 217-243.

[11] Singh MP, Moreschi LM. Optimal placement of dampers for passive response control. *Earthquake Engineering Structural. Dynamics*, 2002; 31, 955-976.

[12] Trombetti T, Silvestri S. Added viscous dampers in shear-type structures: the effectiveness of mass proportional damping. *Journal of Earthquake Engineering*, 2004; 8(2), 275-313.

[13] Zhang RH, Soong TT. Seismic design of viscoelastic dampers for structural applications, *Journal of Structural Engineering-ASCE*, 1992; 118(5), 1375-1392.

[14] Takewaki I, Optimal Damper Placement for Minimum Transfer Functions, *Earthquake Engineering and Structural Dynamics*, 1997; 26(11), 1113-1124, 1997.

[15] Lopez Garcia D. A simple method for the design of optimal damper configurations in MDOF structures, *Earthquake Spectra*, 2001; 17(3), 387-398.

[16] Liu W, Tong M, Wu X, Lee GC. Object-oriented modeling of structural analysis and design with application to damping device configuration, *Journal of Computing in Civil Engineering-ASCE*, 2003; 17(2), 113-122.

[17] Park JH, Kim J, Min KW. Optimal design of added viscoelastic dampers and supporting braces, *Earthquake Engineering and Structural Dynamics*, 2004; 33(4), 465-484.

[18] Lavan O, Levy R. Optimal design of supplemental viscous dampers for linear framed structures, *Earthquake Engineering and Structural Dynamics*, 2006; 35(3), 337-356.

[19] Aydina E, Boduroglub MH, Guney D. Optimal damper distribution for seismic rehabilitation of planar building structures, *Engineering Structures*, 2007; 29(2) 176–185.

[20] Soong TT, Constantinou MC. Passive and active structural vibration control in civil engineering. Springer-Verlag, New York, 1994.

[21] Lee SH, Min KW, Hwang JS, Kim J. Evaluation of equivalent damping ratio of a structure with added dampers. *Engineering Structures*, 2004; 26, 335-346.

[22] Di Paola M, La Mendola L, Navarra G. Stochastic seismic analysis of structures with nonlinear viscous dampers. *Journal of Structural Engineering ASCE*, 133(10), 1475-1478.

[23] Wen YK. Methods of random vibration for inelastic structures. *Applied Mechanics Reviews*. 1989; 42(2), 39-52.

[24] Roberts JB, Spanos PD. Random Vibration and Statistical Linearization. *John Wiley & Sons*., 1990, New York.

[25] Grossmayer RL, Iwan WD. A linearization scheme for hysteretic systems subjected to random excitation, *Earthquake Engineering and Structural Dynamics*. 1981; 9(2), 171–185.

[26] Takewaki, I. Probabilistic critical excitation for MDOF elastic-plastic structures on compliant ground, *Earthquake Engineering and Structural Dynamics*, 2001; 30(9), 1345-1360

[27] Sigaher AN, Constantinou MC. Scissor-jack-damper energy dissipation system, *Earthquake Spectra*, 2003; 19(1), 133–158.

[28] Hwang JS, Kim J, Kim YM. Rotational inertia dampers with toggle bracing for vibration control of a building structure, *Engineering Structures*, 2007; 29(6), 1201–1208

[29] Gluck J, Ribakov Y. Active viscous damping system with amplifying braces for control of MDOF structures. *Earthquake Engineering and Structural Dynamics*, 2002; 31, 1735–1751.

[30] Lee SH, Min KW, Chung L, Lee SK, Lee MK, Hwang JS, Choi SB, Lee HG. Bracing Systems for Installation of MR Dampers in a Building Structure. *Journal Of Intelligent Material Systems And Structures*, 2007, 18(11), 1111-1120.

[31] Hwang JS, Huang YN, Hung YN. Analytical and experimental study of toggle-brace-damper systems, *Journal of Structural Engineering-ASCE*, 2005; 131(7), 1035-1043.

[32] Di Paola M, Ioppolo M, Muscolino G. Stochastic seismic analysis of multidegree of freedom systems. *Engineering Structures*, 1984, 6(2), 113-118.

[33] Di Paola M, Muscolino G. Response maxima od a SDOF system under seismic action. *Journal of Structural Engineering ASCE*, 111(9), 2033-2046.

[34] Vanmarcke EH. Properties of spectral moments with application to random vibration. *Journal of Structural Engineering*-ASCE, 1972; 98(2), 425-446.

[35] Warburton GB, Soni, SR. Error in response calculations for non-classically damped structures. *Earthquake Engineering Structural. Dynamics*, 1977; 5, 365-376.

[36] Federal Emergency Management Agency (FEMA). NEHRP provisions for the seismic rehabilitation of building" *Reps. FEMA 273 (Guidelines) and 274 (Commentary)*, Washington, D.C., 1997.

[37] Commission of European Communities. Eurocode 8, earthquake resistant design of structures. Brussels, Belgium, 2005.

[38] Italian code. Norme Tecniche per le Costruzioni. Decreto Ministeriale 14 settembre 2005. Gazzetta Ufficiale n. 222 del 23 settembre 2005. Supplemento Ordinario n. 159.

[39] Cacciola P, Colajanni P, Muscolino G. Combination of Modal Responses Consistent with Seismic Input Representation. *Journal of Structural Engineering-ASCE,* 2004; 130(1), 47-55.